Fuel 226 (2018) 472–478

Contents lists available at ScienceDirect

Fuel

journal homepage: www.elsevier.com/locate/fuel

Full Length Article

Accessing unconventional biofuels via reactions far from local equilibrium

Yu Gao, Necip B. Uner, Elijah Thimsen*, Marcus B. Foston*

Department of Energy, Environmental & Chemical Engineering, Washington University in St. Louis, 1 Brookings Drive, Saint Louis, MO 63130, USA

GRAPHICAL ABSTRACT

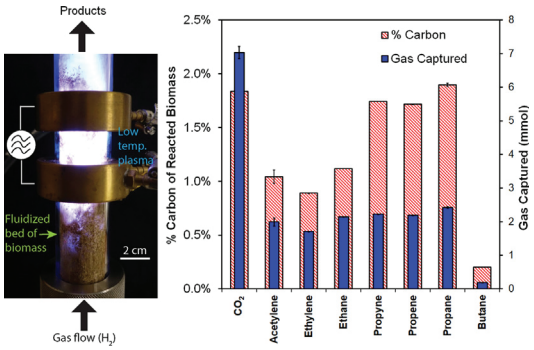

ARTICLE INFO

Keywords:
Non-thermal plasma
Lignocellulose biomass
Fluidized bed

ABSTRACT

The thermochemical production of fuels from lignocellulosic biomass is constrained by equilibrium thermodynamics. However, low temperature plasma reactions are not governed by local equilibrium and involve the formation of unique radical and ion species. Thus, low temperature plasma can open pathways in the conversion of lignocellulosic biomass to products not observed in conventional thermochemical processing. In this effort, a novel radio-frequency (RF) plasma-enhanced fluidized bed reactor was utilized for the low temperature plasma deconstruction of lignocellulosic biomass in a hydrogen background gas. Of the reacted biomass in the plasma, 35% of the carbon was converted into hydrocarbons. Specifically, 16.9, 8.2, 9.6, and 0.2% of the reacted carbon from the biomass was converted into CH_4, C_2H_x, C_3H_x, and C_4H_x, respectively. With increasing power input, more rapid conversion of biomass was achieved, while the total amount of carbon from the biomass converted into hydrocarbons was similar.

1. Introduction

A significant challenge for large-scale biomass utilization is related to the generation of value-added products, *i.e.*, biomass-derived drop-in fuels, chemicals, and materials. Established thermochemical methods of deconstructing biomass, such as gasification and pyrolysis, have the advantage of rapid kinetics and provide possible routes to precursors for the synthesis of such products. Gasification processes (> 1000 K) result in the decomposition of biomass towards an equilibrium composition comprised mainly of CO and H_2, also known as synthesis gas. The conversion of synthesis gas to higher value hydrocarbon products can then be accomplished *via* Fischer–Tropsch chemistry. However, production of Fischer–Tropsch liquids from biomass has not seen widespread commercial deployment [1]. Thermal pyrolysis (~300–900 K) employs similar biomass decomposition pathways that are selected for by lower reaction temperatures and operate under local equilibrium to generate kinetic products such as bio-oil. This bio-oil product is a heterogeneous mixture of acids, alcohols, aldehydes, esters,

* Corresponding authors.
E-mail address: mfoston@wustl.edu (M.B. Foston).

https://doi.org/10.1016/j.fuel.2018.03.188
Received 1 February 2018; Received in revised form 28 March 2018; Accepted 29 March 2018
Available online 13 April 2018

ketones, sugars, phenols, guaiacols, syringols, and furans, which must then undergo several subsequent resource-intensive upgrading processes, such as hydrodeoxygenation, before the products resemble precursors useful in the production of fuels [2].

A major challenge with thermochemical processing of biomass is that known processes generate either a product of little direct value (*e.g.,* synthesis gas *via* gasification) or a heterogeneous mixture with low selectively for any given species (*e.g.,* bio-oil). Developing a biomass conversion method that benefits from the same advantageous kinetics observed for thermochemical processing but affords direct access to more commercially valuable product distributions would be tremendously useful. However, that goal represents a major technical challenge (*vide infra*).

Plasmas are ionized gases that can be classified into two main groups: high and low temperature. High temperature plasmas, or thermal plasmas, are characterized by electrons, ions, and neutrals being in *local thermal equilibrium* at a very high temperature, typically in excess of 3000 K. On the other hand, low temperature plasmas are a non-equilibrium substance wherein *local equilibrium cannot be assumed*. For example, the heavy species in a low temperature plasma, such as neutral gas molecules and ions, are typically $T < 1000$ K, but the free electrons are very hot, often $T_e > 20{,}000$ K. In other words, temperatures of species in a low temperature plasma may be different by an order of magnitude at the same location in space. The very hot electrons cause a plethora of reactive kinetically-controlled processes when collisions occur with neutral gas molecules and surfaces. Examples of such reactive process include: electron impact dissociation or excitation, spontaneous photoemission, ionization, etc. [3]. These highly energetic kinetic processes are expected to deconstruct biomass easily. Also, many of the reactions occurring during deconstruction of biomass are known to involve radical and ionic intermediates [4,5]. Unique radicals and ions may be generated in low temperature plasma that open pathways with rapid kinetics to products that are inaccessible via conventional thermochemical routes governed by local equilibrium. Moreover, from the perspective of thermodynamics, low temperature plasma processes must obey the 1st and 2nd laws; however, the product distributions resulting from plasma processes are not constrained by equilibrium thermodynamics. In fact, low temperature plasmas are capable of moving chemical systems away from equilibrium. For example, it has been observed that when pure CO_2 is fed into a low temperature plasma at conditions where it is the thermodynamically stable species of carbon, it can be split and significant quantities of CO are formed with carbon mole fraction of approximately 70% [6]. Additionally, it is well known that if pure O_2 is fed into low temperature plasma, the effluent may contain a mole fraction of up to 10% O_3, which is again a move away from equilibrium [7]. Due to these alluring features, low temperature plasmas have begun to attract attention for processing biomass. The focus in this paper is on converting the biomass into hydrocarbons, which are useful as polymer precursors (*e.g.,* ethylene) or transportation fuels (*e.g.,* propane and butane).

Vanneste et al. recently published a review on the application of low temperature plasma for pretreatment of lignocellulose [8]. There are published examples of biomass deconstruction by low temperature plasma, but knowledge of product distributions is limited [8–12]. There have been a few published studies that do detail the product distributions generated in high temperature thermal plasmas [13–16]. Typical product distributions from these high temperature systems governed by local equilibrium are similar to thermal gasification of biomass with approximately 65 wt% yields of gas, principally comprised of CO and H_2, and the remainder of carbon in the form of char. Summaries within studies by Shie et al. [11] and Huang et al. [14] concisely review research conducted on plasma-based pyrolysis and gasification technologies, demonstrating the opportunity for more detailed study. Accordingly, for low temperature plasmas in which local equilibrium cannot be assumed, there remains a large number of gaps in knowledge about the biomass processing application.

In this work, a low temperature plasma was used to deconstruct lignocellulosic biomass in a hydrogen background gas. To improve the plasma-biomass contact area, a low temperature plasma-enhanced fluidized bed reactor was utilized. In the plasma reactor, switchgrass was reacted and a significant fraction of the carbon atoms fed into the plasma reacted to form hydrocarbons. The distribution of these hydrocarbons contained a significant fraction of methane, but contained also heavier species such as propane and butane.

2. Materials and methods

2.1. Chemicals

Switchgrass (*Panicum virgatum*; Wiley milled and sieved 80 to 20-mesh fraction; James R. Frederick, Pee Dee Research and Education Center, Clemson University, Florence, SC) was Soxhlet extracted with ethanol:toluene (2:1) and then water overnight. All gases were purchased from Airgas and all reagents were purchased from Sigma-Aldrich.

2.2. Plasma-enhanced fluidized bed reactor (PEFBR)

The reactor employed in this study is unique in the sense that it is capable of homogenously treating 10–100 g scale biomass by direct plasma contact. In a recent review, Vanneste et al. noted that a dynamic high-throughput reactor for uniform plasma treatment of biomass is a major challenge for potential industrial application [8]. The plasma-enhanced fluidized bed reactor (PEFBR) exactly fulfils these needs because of the constant mixing of solids provided by fluidization. Low pressure operation provides a large plasma volume, and ensures good contact between the particles and the plasma. Furthermore, using RF power and the placement of the electrodes outside of the reactor prevents electrode contamination and provides robust operation.

The PEFBR is a batch system comprised of a reaction zone, a liquid nitrogen trap for collection of condensable species, and a quadruple mass spectrometer (QMS) for online measurement of the effluent composition. A schematic of the system is presented in Fig. 1a. The reactor consisted of a vertical fused silica tube of 120 cm height and 3.8 cm outer diameter. A quantity of 22.2 g of dried switchgrass (35–50 mesh size) was loaded in to the reactor. The switchgrass rested on a sintered metal filter that acted as a flow distributer. Switchgrass particles were found to be difficult to fluidize since they are light and prone to channeling. To enhance fluidization and prevent channeling, 30 g of 400–600 μm diameter glass beads, which were assumed to be chemically inert, were added to the reactor. A second sintered metal filter was placed on the outlet of the fused silica tube to prevent elutriation of fine particles into the vacuum system. The system was pumped down, and then a constant flow of 600 standard cubic centimeters per minute (sccm) of grade 5.0 H_2 was flowed upwards, causing the mixture to fluidize. The pressure measured upstream of the bottom sintered metal filter was 3.2 kPa and downstream of the top sintered metal filter was 1.7 kPa. The average of these values was taken as the reaction pressure of 2.5 kPa. Plasma was generated by coupling radio frequency power (13.56 MHz) to two brass ring electrodes around the tube. The electrodes were water cooled and they were placed just above the bed. Unless otherwise stated, the applied power was 275 W. The bed fluidized in a slugging regime and plasma was generated in the large gas bubbles within the bed, forming a reaction zone with an approximate power density of a few W cm^{-3} (see Fig. 1b).

The effluent from the PEFBR was passed through a liquid nitrogen trap to collect condensable species. The liquid nitrogen trap had valves on the inlet and outlet, and thus, it could accommodate positive pressures up to 100 psi, allowing for the condensed products, some of which had boiling points below room temperature, to warm up safely to room temperature after the reaction was complete. The lines between the reaction zone and the liquid nitrogen trap were maintained at room

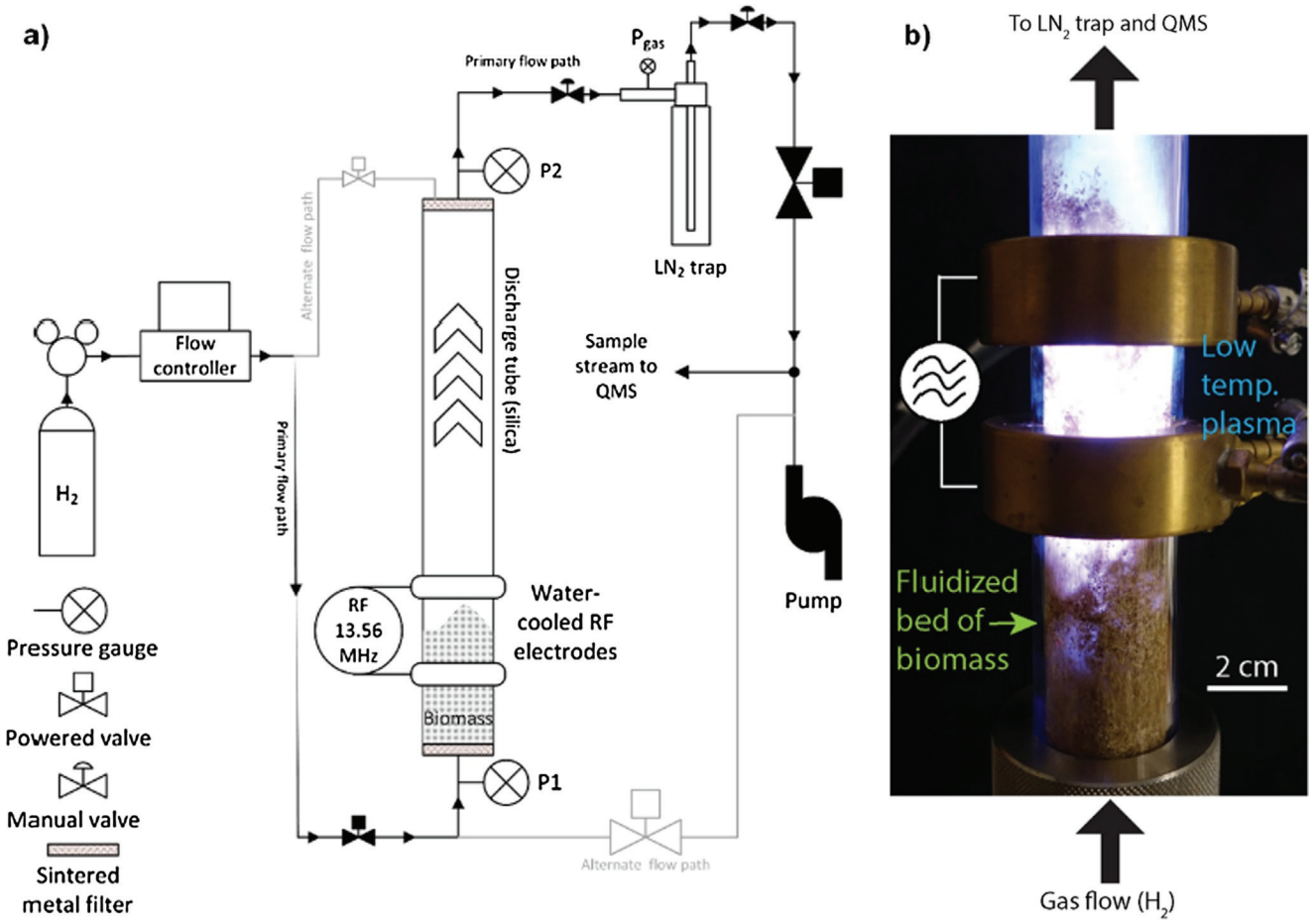

Fig. 1. Experimental apparatus. (a) Schematic of the system and (b) digital photograph of plasma reaction zone during biomass deconstruction.

temperature. The contents of the cold trap were analyzed using gas chromatography–mass spectroscopy (GC–MS). The light species that passed through the trap were quantified online using a quadrupole mass spectrometer (QMS, ExTorr XT300) in the *m/z* range from 1 to 300 AMU. The residual solid mass was collected from the reactor and massed after the reaction.

2.3. Gas chromatography–mass spectroscopy on cold trapped gas products

Gas sample for GC–MS analysis was prepared by expanding the products from the trap into an inverted graduate cylinder under room temperature and pressure. A quantity of 50 μL of this raw gas mixture was injected into a nitrogen purged dilution flask (1000 mL). The diluted gas was left to reach equilibrium for 10 min. An amount of 200 μL of this diluted gas was manually injected on an Agilent GC system 7890A coupled with Agilent 5975C mass spectroscopy with triple-axis detector. GC analysis was performed using an Agilent J&W GS-CarbonPLOT capillary column (ID: 0.32 mm, film thickness: 3 μm, and length: 60 m) with the following program: 2 min at 308 K, ramped at 5 K/min up to 393 K, and then ramped 25 K/min up to 623 K for a total time of 28.2 min under SIM mode with helium as a carrier gas (splitting ratio: 2:1). To quantify the gas yields, calibration curves of C2-C4 hydrocarbons were produced using the standard gas mixture comprising CH_4, C_2H_2, C_2H_4, C_2H_6, C_3H_4, C_3H_6, C_3H_8, and C_4H_{10} in nitrogen and calibration curves of CO_2 were produced using the standard gas mixture comprising CO, CO_2, CH_4, C_2H_2, C_2H_4, and C_2H_6 in nitrogen (custom-mixed by Scott Specialty Gases, Plumsteadville, PA). GC–MS data was exported and analyzed through ChemStation software.

2.4. Gas chromatography–mass spectroscopy on cold trapped liquid products

GC–MS sample of liquid products was prepared from organic extraction on 1 mL of liquid products directly collected from the trap by using 1 mL of chloroform in a centrifuge tube. Mixture was vortexed for three times (10 s each time) and the organic phase was collected. Extraction was performed three times and the organic phased was combined. Decane was added into the organic phase as an internal standard. A quantity of 1 μL of GC–MS sample was injected on a modified Agilent GC system 7890A coupled with both an Agilent 5975C mass spectroscopy with triple-axis detector and an Agilent G3461A FID with methanizer (Activated Research Company) through an Agilent G3470A Auxiliary Electronic Pressure Control (Aux EPC). GC analysis was performed using an Restek fused silica RTX-50 capillary column (ID: 0.25 mm, film thickness: 0.5 μm, and length: 30 m) with the following program: 2 min at 313 K and then ramped at 5 K/min up to 573 K for 5 min with helium as a carrier gas (splitting ratio: 10:1). GC–MS data was exported and analyzed through ChemStation software. Identification of the compounds was carried out by comparing the mass spectra obtained with these from system database (PAL600k, Palisade Corporation, USA).

2.5. Total organic carbon on feedstock and residual biomass

Total carbon content in starting switchgrass, solid residues remaining after deconstruction, and liquid products collected in the cold trap was determined by using a Solid Sample Module Shimadzu Carbon Analyzer (SSM-5000A) operated at 1173 K with an oxygen flowrate of 0.5 L/min. Analysis was first calibrated by using sucrose as a standard.

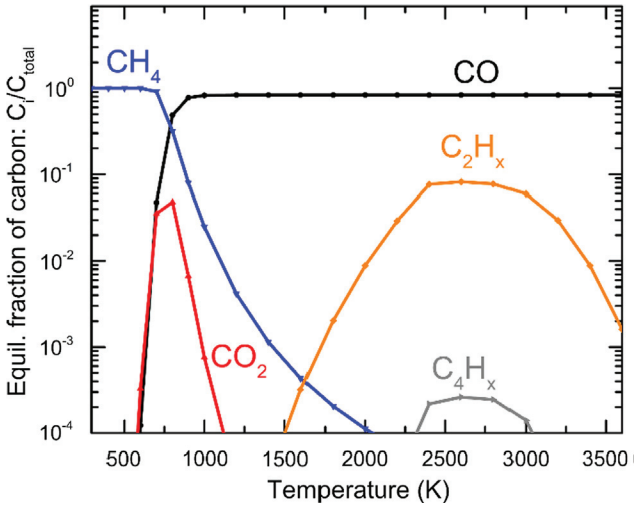

Fig. 2. Equilibrium speciation of carbon in a system initially charged with 20 g of $C_6H_{10}O_5$ and 17.5 g of H_2 at a constant pressure of 2.5 kPa calculated using the NASA CEA code [17]. Elemental carbon is not shown on the plot for the sake of clarity. Elemental carbon accounts for the balance of carbon at high temperatures. A total of 131 species were considered in the equilibrium calculations, including hydrocarbon chains up to 12 carbons in length.

Each sample was measured in three replicates and their average was used in the report of this work.

3. Results and discussion

Before presenting results, the expected behavior of the system is described from the perspective of equilibrium thermodynamics. Such a description is necessary to understand if any unexpected phenomena have occurred. A system in equilibrium at constant temperature and pressure, initially charged with biomass and excess hydrogen would produce CH_4 at low temperatures and CO at more elevated temperatures. Specifically, the equilibrium speciation of carbon initially charged with 20 g of cellulose and 17.5 g of hydrogen at a constant pressure of 2.5 kPa (to match experimental conditions used in this work) was calculated using NASA's CEA code [17] and plotted as a function of temperature in Fig. 2. At low temperatures, the direction of the reaction is promising as it proceeds towards the thermodynamic product of CH_4. However, for thermochemical processing governed by local equilibrium, at low temperature, bio-oil is produced (presumably a kinetically arrested intermediate). At high temperature, the system will produce a gas tending towards CO. However, for decomposition of biomass in low temperature plasmas, an expectation of what reaction pathways will be favored is difficult to form, since the local equilibrium assumption cannot be made.

The switchgrass was deconstructed by the plasma in the reactor for several hours. During the deconstruction, the wall temperature of the discharge tube between the brass electrodes was estimated to be approximately 600 K by using an infrared camera, which can be taken as a rough estimate of the neutral gas temperature. A total of 17.5 g of hydrogen were fed into the reactor, as determined by the set point on the mass flow controller, and a total of 16.0 g of hydrogen were detected in the reactor effluent by the in-situ QMS. Therefore, an estimated 1.5 g of hydrogen were consumed by the reaction. The liquid nitrogen trap was found to be very effective for collecting large molecules and water produced by the reaction; however, a significant fraction of the lighter hydrocarbons, CO, and CO_2 passed through. These lighter species were quantified online using the QMS. During the biomass deconstruction reaction, a total of 11 g of the biomass reacted and was removed from the bed, as determined by measuring the mass and total carbon in the residual solid mixture remaining in the reactor bed following the experiment.

The carbon content of the starting and residual biomass remaining after the reaction was quantified by total organic carbon (TOC) analysis. A total of 787.9 mmol of carbon were fed into the reactor, of which 383.7 mmol reacted (*i.e.*, 49% conversion by TOC). Photographs of the starting biomass and the residual biomass remaining in the reactor bed after low temperature plasma deconstruction is shown in Fig. 3. Importantly, the residual biomass is visually very different than

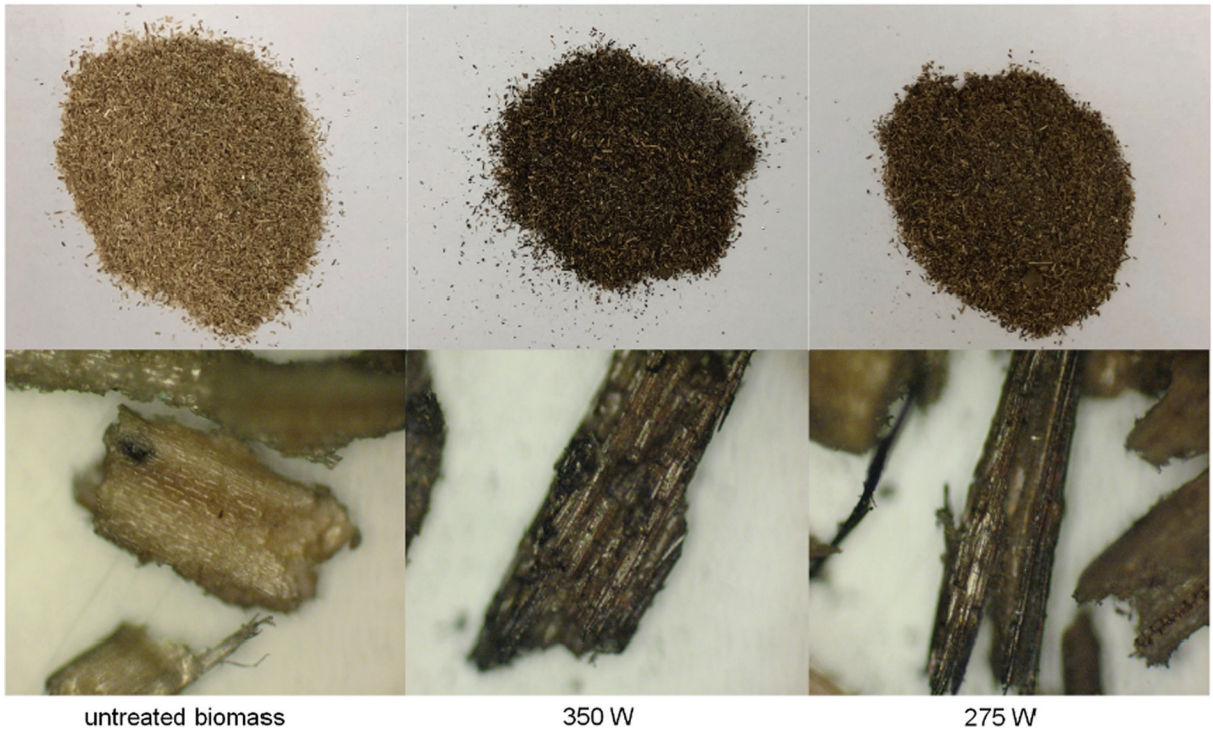

Fig. 3. Starting and residual biomass remaining in the reactor bed after deconstruction with low temperature plasma.

Table 1
Product distribution. A total of 787.9 mmol of carbon were fed into the reactor, of which 383.7 mmol reacted. The amount of carbon collected in the liquid phase was 4.88 mmol. The amount of various carbonaceous gases produced by the reaction are summarized in the table below. The percentages are the fraction of reacted carbon that formed the various species.

Product	mmol carbon	% of Reacted biomass
CO_2	17.0	4.4%
CO	22.8	5.9%
CH_4	65.0	16.9%
C_2H_x	31.3	8.2%
C_3H_x	37.0	9.6%
C_4H_x	0.8	0.2%
Liquid	4.88	1.3%

the typical char associated with thermochemical processing (*e.g.*, torrefaction or pyrolysis). In fact, the solid state nuclear magnetic resonance (NMR), thermogravimetric (TGA), and chemical cell wall analyses conducted on the starting and residual biomass suggest that much of the residual biomass is in fact unreacted biomass (see Figs. A1, A2, and Table A1). The visual appearance and these chemical analyses of the residual biomass suggest that biomass particles are degraded in the plasma from its surface and the only chemically altered biomass is at the surface of a particle. Therefore, longer residences times for the biomass particle in the plasma would have likely led to higher conversions. Also, the liquid collected in the trap after the low temperature plasma deconstruction of biomass was analyzed by TOC analysis. The amount of carbon collected in the aqueous liquid phase was ~4.88 mmol of carbon. The gases and liquids collected in the trap were analyzed offline by GC–MS. By also quantifying the amount of carbon that was collected in the trap and the carbon detected by the QMS, it was possible to determine the fraction of reacted carbon that formed each of the various products as summarized in Table 1.

The QMS data revealed that the rate of gaseous product generation was fairly steady and significant amounts of gaseous products passed through the liquid nitrogen trap. Partial pressures for select *m/z* values were recorded continuously as a function of time, specifically *m/z* values of 2, 15, 26, 28, 41, and 44; used to monitor H_2, CH_4, C_2H_2, CO, C_3H_x, and CO_2, respectively. The signal from the QMS was calibrated by comparing to a known flow rate to obtain a constant of proportionality that related the signal to the flow rate of a given species. The signal during reaction was then baselined and multiplied by the calibration factor to obtain the flow rate of various species in the reactor effluent as a function of time. The flow rate of select species, as measured by QMS, is plotted in Fig. 4. The flow rate of condensable species showed an oscillatory pattern, which was caused by a slight release of product from the trap when the level of liquid nitrogen was low; followed by a decrease when the operator refilled the dewar for the trap approximately every 15 min. The methane, on the other hand, showed a steady production rate since it was not condensable at liquid nitrogen temperature. The flow rates of the products were fairly constant over the course of the reaction, showing only a variation near the end. The total amount produced for each of the species over the course of the reaction, which was not collected in the liquid nitrogen trap, was determined by integrating the curves in Fig. 4. QMS as practiced here is convenient, but unfortunately not completely definitive. To be more quantitative, GC–MS was performed on the material collected in the trap.

After allowing the trap to warm up, the majority of the carbon collected was present as a gas at room temperature. At ambient conditions, 450 cm^3 of gas was extracted from the trap; as well as 2.0 mL of a brown aqueous liquid. The chromatogram of the gas is presented in Fig. 5a and the quantification in Fig. 5b. The carbon in the gas was mostly present as deoxygenated C2 and C3 hydrocarbons; in addition to a small amount of carbon dioxide. The GC–MS analysis of the gas extracted from the trap agrees with the interpretation of the QMS

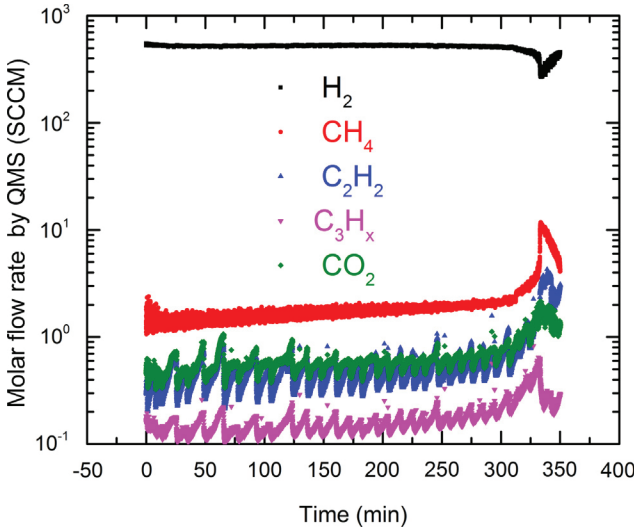

Fig. 4. Composition of effluent during reaction. Molar flow rate measured by QMS, downstream of the liquid nitrogen trap, as a function of time. The curves are labeled as H_2 (black) CH_4 (red), acetylene (blue), C3 hydrocarbons (*e.g.*, propyne, propene and propane, magenta) and CO_2 (green). (For interpretation of the references to colour in this figure legend, the reader is referred to the web version of this article.)

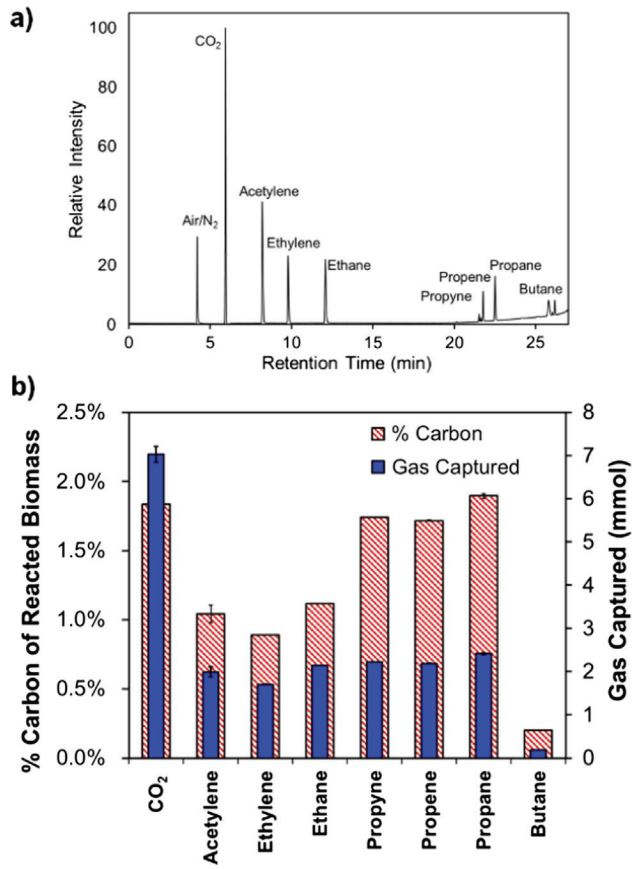

Fig. 5. Analysis of gas collected from liquid nitrogen trap. (a) Chromatogram showing clear resolution of various C2 and C3 hydrocarbons. (b) Quantification of the amount of each of the gaseous species collected in the trap. The grey bars are the number of mmols of each gaseous species collected in the trap. The red bars are the fraction of carbon from the reacted biomass that was transformed into each of the species. Error bars represent analytical replicates. (For interpretation of the references to colour in this figure legend, the reader is referred to the web version of this article.)

measurements in Fig. 4. By combining the QMS measurement and the GC–MS quantification of the gas extracted from the trap, the total amount of the gaseous products can be calculated. The amount of carbon atoms that formed CO_2, CO, CH_4, C_2H_x, C_3H_x and C_4H_x from the reacted biomass are tabulated in Table 1. Table 1 shows that approximately 45.2% of the carbon in the reacted biomass formed gaseous products *that were detected*. That conversion is similar to previous reports on plasma conversion of biomass [14–16]. The key difference is the product distribution – specifically the large relative abundance of hydrocarbons (*i.e.*, methane, C_2H_x, and C_3H_x). The relatively high selectivity for C3 hydrocarbons, in particular, is interesting since those compounds are not expected at equilibrium for any temperature (Fig. 2).

In the present work, at a reactor wall temperature of approximately 600 K in the presence of hydrogen, low temperature plasma deconstruction of biomass generated a product that was at least 45% gas, and ~45% of that gas was hydrocarbon species containing multiple carbon atoms (*i.e.,* C2, C3, and C4 hydrocarbon species). In an effort to determine whether the observed product distribution generated from biomass using a low temperature plasma is different than that obtained using thermochemical processing, consider several pyrolysis and hydropyrolysis studies (Table 2). Rocha et al. conducted pyrolysis on cellulose with a hydrogen pressure of 0.5 MPa at 573 K and generated a product composed of about 1% gas, 9% bio-oil, and 90% char. At a higher temperature of 623 K in that same report, a product was generated comprised of about 5% gas, 35% bio-oil, and 40% char [18]. Pilon et al. preformed pyrolysis of switchgrass in nitrogen environments at 573 K generating a product composed of about 21% gas, but that only contained 0.1% C2, C3, or C4 hydrocarbons [19]. At 673 K, Pilon et al. found that the pyrolysis of switchgrass generated a product composed of about 27% gas and contained 0.6% C2, C3, and C4 hydrocarbons. Therefore, this work demonstrates the highly selective production of gaseous C2, C3 and C4 hydrocarbons when compared to previous reports of thermochemical processing.

The brown liquid generated by the plasma reaction and collected in the liquid nitrogen trap was a hydrophilic liquid (immiscible in hexane, chloroform, and ethyl acetate), most likely water, with a carbon content based on TOC analysis of 1.3% of the reacted biomass. ^{1}H NMR of the liquid confirmed that ~90% of the protons in the sample were related to water (see Fig. A3). GC–MS analysis of the product extracted from the liquid using chloroform revealed the presence of a wide distribution of compounds (see Fig. A4). The most prevalent compounds detected were various cyclic and linear ketones presumably from the decomposition of carbohydrates and phenolics from the decomposition of lignin. The carbon content of GC-detectable compounds (based on analysis by a GC-methanizer and flame ionization detector) was ~0.5% of the reacted biomass, indicating that more than half the carbon in the liquid product was either insoluble in chloroform or oligomeric in nature. A full list of compounds detected by GC–MS analysis was generated (see Table A2). The presence of the small molecules detected in the liquid phase suggests that biomass deconstruction with low temperature plasma may proceed through these oxygenated intermediates.

Of the products analyzed, methane was present in the largest fraction (Table 1). One interpretation of the results is that the system is tending towards the equilibrium state at the reactor temperature (*i.e.,* 600 K), although displaying much more rapid kinetics than are observed in thermochemical systems. The C2, C3, and C4 hydrocarbons could be considered as kinetic intermediates on the path from biomass to methane. Indeed, the observation of approximately equal amounts of CO_2 and CO, which are both small with respect to the hydrocarbons, is consistent with the interpretation of an equilibrium state being approached at an effective temperature slightly less than the crossover between CH_4 and CO dominance (Fig. 2). To test whether this interpretation was reasonable, an additional experiment was conducted.

An experiment was conducted wherein all conditions were kept the same, except the power was increased from 275 W to 350 W. The reaction was carried out for a sufficient amount of time that approximately the same number of moles of carbon reacted, as determined by TOC analysis. With the increase in power came an increase in the ion density in the plasma [20] as well as an increase in gas temperature. Thus, if the 275 W experiment was already at the border between CH_4 and CO dominance, then the 350 W experiment is expected to show: 1) more rapid conversion of biomass and 2) product distribution more similar to the higher temperature region of Fig. 2. More rapid conversion of biomass was achieved, indeed the rate of biomass conversion increased from ~1.8 g h^{-1} to ~2.8 g h^{-1} with the increase in power. Furthermore, the amount of CO produced at 350 W was significantly higher compared to 275 W, and greater than the amount of methane (Fig. 6). Interestingly, the total amount of carbon present as hydrocarbons was similar for both powers, 133 mmol at 275 W and 119 mmol at 350 W. The increase in the amount of CO relative to CH_4 with power is consistent with an increase in neutral gas temperature; however, the observation that the total amount of carbon present as hydrocarbons remained constant contradicts the idea of the system approaching an equilibrium state at a higher temperature for 350 W compared to 275 W. There appeared to be some dependence of the hydrocarbon product distribution on the external process parameters (Fig. 6). There may be an opportunity to synthesize even longer chain hydrocarbons by judiciously controlling residence time in a different reactor configuration; or by controlling the gas temperature through external cooling.

Table 2
Example data for the plasma and conventional pyrolysis of biomass (blank entry means data not available).

Conversion Technology	Gas Yield	Liquid Yield (%)	Char Yield (%)	Gas Product Hydrocarbon Content (vol%)	Ref.
High Temp Plasma	38%		61		[9]
High Temp Plasma	85%				[10]
Low Temp Plasma	885 mL/g			3.9	[14]
Low Temp Plasma	60%			7.6	[15]
Low Temp Plasma	79%			8.6	[16]
Pyrolysis (300 °C, 300 °C/min, 10 min)	0%	10	90		[18]
Hydropyrolysis (300 °C, 55 °C/min, 2 min)	20%	25	60	0.4	[19]
Current Study	45%	0.6	1.6	30	

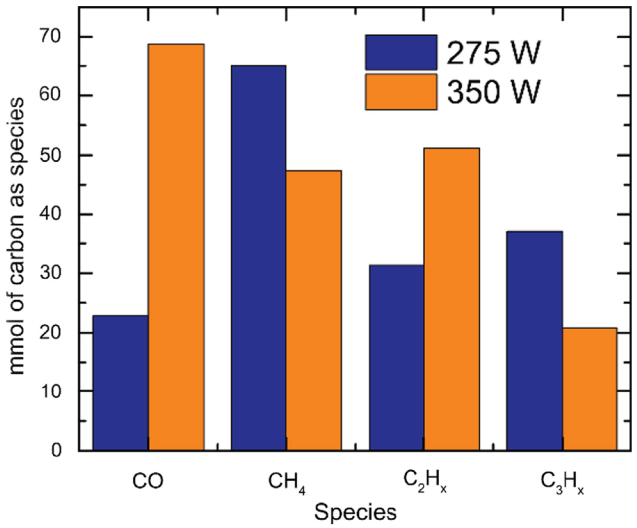

Fig. 6. Product distribution for two different applied RF powers. In both cases, the amount of reacted biomass was approximately the same.

4. Conclusions

An exploratory study of biomass deconstruction by a low temperature fluidized bed reactor in hydrogen background gas demonstrated a significant yield of hydrocarbons. At least 35% of the carbon from the reacted biomass formed methane, C2, and C3 compounds. There is evidence that through kinetic controls and manipulating external process parameters, the product distribution can be adjusted to access even larger hydrocarbons. Future efforts will utilize new reactor designs better suited to biomass conversion and for controlling residence times in the plasma.

Acknowledgements/funding

This work was partially supported by the Consortium for Clean Coal Utilization (CCCU) at Washington University in St. Louis; the National Science Foundation (NSF) under grant agreement PHY-1702334; and the Center for Engineering MechanoBiology (CEMB), an NSF Science and Technology Center, under grant agreement CMMI: 15-48571.

Appendix A. Supplementary data

Supplementary data associated with this article can be found, in the online version, at http://dx.doi.org/10.1016/j.fuel.2018.03.188.

References

[1] Spath P, Dayton D. Preliminary screening - technical and economic assessment of synthesis gas to fuels and chemicals with emphasis on the potential for biomass-derived syngas NREL Technical Report NREL/TP-510-34929 2003.
[2] Mohan D, Pittman CU, Steele PH. Pyrolysis of wood/biomass for bio-oil: a critical review. Energy Fuels 2006;20(3):848–89.
[3] Nehra V, Kumar A, Dwivedi H. Atmospheric non-thermal plasma sources. Int J Eng 2008;2(1):53–68.
[4] Mettler MS, Vlachos DG, Dauenhauer PJ. Top ten fundamental challenges of biomass pyrolysis for biofuels. Energy Environ Sci 2012;5(7):7797–809.
[5] Demirbaş A. Mechanisms of liquefaction and pyrolysis reactions of biomass. Energy Convers Manage 2000;41(6):633–46.
[6] Brown LC, Bell AT. Kinetics of the oxidation of carbon monoxide and the decomposition of carbon dioxide in a radiofrequency electric discharge. I. Experimental results. Ind Eng Chem Fundam 1974;13(3):203–10.
[7] Eliasson B, Hirth M, Kogelschatz U. Ozone synthesis from oxygen in dielectric barrier discharges. J Phys D Appl Phys 1987;20(11):1421.
[8] Vanneste J, Ennaert T, Vanhulsel A, Sels BF. Unconventional pretreatment of lignocellulose with low temperature plasma. ChemSusChem 2016.
[9] Tang L, Huang H. Plasma pyrolysis of biomass for production of syngas and carbon adsorbent. Energy Fuels 2005;19(3):1174–8.
[10] Du C, Wu J, Ma D, Liu Y, Qiu P, Qiu R, et al. Gasification of corn cob using non-thermal arc plasma. Int J Hydrogen Energy 2015;40(37):12634–49.
[11] Shie J-L, Chang C-Y, Tu W-K, Yang Y-C, Liao J-K, Tzeng C-C, et al. Major products obtained from plasma torch pyrolysis of sunflower-oil cake. Energy Fuels 2007;22(1):75–82.
[12] Tu W-K, Shie J-L, Chang C-Y, Chang C-F, Lin C-F, Yang S-Y, et al. Pyrolysis of rice straw using radio-frequency plasma. Energy Fuels 2007;22(1):24–30.
[13] Hlina M, Hrabovský M, Kopecký V, Konrad M, Kavka T, Skoblja S. Plasma gasification of wood and production of gas with low content of tar. Czech J Phys 2006;56:B1179–84.
[14] Huang H, Tang L. Treatment of organic waste using thermal plasma pyrolysis technology. Energy Convers Manage 2007;48(4):1331–7.
[15] Diaz G, Sharma N, Leal-Quiros E, Munoz-Hernandez A. Enhanced hydrogen production using steam plasma processing of biomass: experimental apparatus and procedure. Int J Hydrogen Energy 2015;40(5):2091–8.
[16] Zhao Z, Huang H, Wu C, Li H, Chen Y. Biomass pyrolysis in an argon/hydrogen plasma reactor. Eng Life Sci 2001;1(5):197–9.
[17] McBride B, Zehe M, Gordon S. Glenn coefficients for calculating thermodynamic properties of individual species NASA TP-2002-211556 2002.
[18] Rocha JD, Luengo CA, Snape CE. The scope for generating bio-oils with relatively low oxygen contents via hydropyrolysis. Org Geochem 1999;30(12):1527–34.
[19] Pilon G, Lavoie J-M. Pyrolysis of switchgrass (*Panicum virgatum L.*) at low temperatures within N_2 and CO_2 environments: product yield study. ACS Sustainable Chem Eng 2012;1(1):198–204.
[20] Roth C, Oberbossel G, von Rohr PR. Electron temperature, ion density and energy influx measurements in a tubular plasma reactor for powder surface modification. J Phys D Appl Phys 2012;45(35):355202.